sations on level crossing in hydrogen with David R. Herrick and with Gregory Hatton.

*This work was supported by U. S. Air Force Office of Scientific Research Contract No. F44620-72-C-0057 and by Joint Services Electronics Program Contract No. DAAB07-75-C-1346.

[1]H. A. Bethe and E. E. Salpeter, *Quantum Mechanics of One- and Two-Electron Atoms* (Academic, New York, 1957).

[2]Recent theoretical work on field ionization in hydrogen: M. H. Rice and R. H. Good, Jr., J. Opt. Soc. Am. 52, 239 (1962); D. S. Bailey, J. R. Hiskes, and A. C. Riviere, Nucl. Fusion 5, 41 (1965); B. M. Smirnov and M. I. Chibisov, Zh. Eksp. Teor. Fiz. 49, 841 (1965) [Sov. Phys. JETP 22, 585 (1966)]; J. O. Hirschfelder and L. A. Curtiss, J. Chem. Phys. 55, 1395 (1971); N. A. Guschina and V. K. Nikulin, Chem. Phys. 10, 23 (1975); L. B. Mendelsohn, Phys. Rev. 176, 90 (1968); M. Alexander, Phys. Rev. 178, 34 (1969); J. Fauchier and J. D. Dow, Phys. Rev. A 9, 98 (1974); M. Hehenberger, H. V. McIntosh, and E. Brändas, Phys. Rev. A 10, 1494 (1974); D. R. Herrick, to be published.

[3]Review articles on field ionization experiments in fast beams: A. C. Riviere, in *Methods of Nuclear Physics*, edited by B. Bederson and W. L. Fite (Academic, New York, 1968), p. 208; R. N. Il'in, in *Atomic Physics 3*, edited by S. J. Smith and G. K. Walters (Plenum, New York, 1973), p. 309.

[4]For example, T. W. Ducas, M. G. Littman, R. R. Freeman, and D. Kleppner, Phy. Rev. Lett. 35, 366 (1975); R. F. Stebbings, C. J. Latimer, W. P. West, F. B. Dunning, and T. B. Cook, Phys. Rev. A 12, 1453 (1975).

[5]Bailey, Hiskes, and Riviere, Ref. 2.

[6]Rice and Good, Ref. 2.

[7]J. E. Bayfield and P. M. Koch, Phys. Rev. Lett. 33, 258 (1974); P. M. Koch, thesis, Yale University, 1974 (unpublished).

[8]M. G. Littman, M. L. Zimmerman, T. W. Ducas, R. R. Freeman, and D. Kleppner, Phys. Rev. Lett. 36, 78 (1976).

[9]W. E. Lamb, Phys. Rev. 85, 259 (1952).

[10]D. Kleppner, in *Atomic Physics and Astrophysics*, edited by M. Chrètien and E. Lipworth (Gordon and Breach, New York, 1971).

Observation and Simulation of Effects on Parylene Disks Irradiated at High Intensities with a 1.06-μm Laser

W. C. Mead, R. A. Haas, W. L. Kruer, D. W. Phillion, H. N. Kornblum, J. D. Lindl, D. R. MacQuigg, and V. C. Rupert

Lawrence Livermore Laboratory, University of California, Livermore, California 94550

(Received 3 May 1976)

Parylene (C_8H_8) disks have been irradiated with a 1.06-μm laser at fluxes of 10^{15}–10^{17} W/cm^2. The spatial and temporal scattered light distributions, x-ray spatial and spectral emission properties, and ion spatial and energy distributions were measured. The results, together with two-dimensional magnetohydrodynamic code simulations, imply absorption via collective processes, laser generation of suprathermal electrons, and transport inhibition consistent with the presence of megagauss-level thermoelectric magnetic fields.

Recent experiments using Nd-glass lasers to heat DT filled glass microspheres suggest that light absorption, plasma heating, and electron conduction play determining roles in achieving compression and thermonuclear neutron production.[1] In order to investigate these processes in simpler systems, many workers have employed plane target geometry.[2]

In the present work,[3] a series of irradiations of parylene-N[4] disks were performed at the JANUS laser facility.[5] The 150-μm-diam by 10-μm-thick C_8H_8 disks were mounted on glass stalks, placed at varying positions with respect to the system's best focus, and irradiated with energies of 6–12 J, and durations of 60–120 psec. Nominal target-spot diameters of 90, 30, and 10 μm were used to cover the intensity range of 10^{15}–10^{17} W/cm^2. An extensive diagnostic package observed plasma behavior on each shot, and detailed comparisons have been made between observations and two-dimensional computer simulations.

The threshold for target damage by prepulse energy was established by using only the oscillator and preamplifiers to apply low-energy pulses to the target. Detailed target inspection showed no observable damage at energy densities below 4.5 J/cm^2. The laser prepulse diagnostic detection limit (2–5 μJ) was sufficiently low to assure no

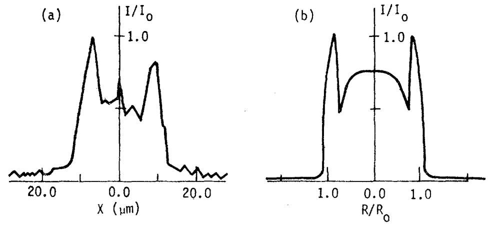

FIG. 1. Beam spatial intensity profiles: (a) measured using multiple image camera; (b) input to simulations.

prepulse target damage at all but the 10-μm spot size. The effect of amplified spontaneous emission on the target was tested by pumping the entire laser system at full gain with the oscillator output blocked. No target damage was evident.

The time-integrated laser energy distribution was measured using a self-calibrating multiple-image camera. Figure 1(a) shows an intensity scan obtained in the image plane with average diameter 27 μm for a shot with 160-GW laser output power. Small-scale self-focusing produced rapid time- and space-varying modulations across the beam. The small target used in these experiments allowed direct observation and control of the amount of incident energy rendered nonfocusable by small-scale self-focusing. Whole-beam self-focusing produced a ring-shaped caustic at the rim of the beam, and a power-dependent shift of the focal spot towards the focusing lens. This was measured to be 3–5 μm at 100 GW, which does not cause difficulty, except for a significant beam size uncertainty at the 10-μm target-spot diameter. Astigmatism caused by the tilted laser disks caused respective beam ellipticities of about 1.1 and 1.5 for the 90- and 30-μm spot

On each shot, the light energy absorbed by the plasma was deduced from measurements of the scattered light using a combination of calorimeters and calibrated photodiodes (which viewed the target through 100-Å bandpass filters). An enclosing calorimeter was used in place of the photodiodes on some shots as an alternative method of obtaining an optical energy balance. The x-ray emission spectrum was determined by using a lead-stearate bent crystal spectrometer (0.3–0.9 keV) and a nine-channel K-edge filter spectrometer (1.5–88 keV). Both detectors were at an angle of $\theta = 135°$ from the incident beam direction. An iterative unfold was used to infer an x-ray spectrum from the known filter bandpass properties of the K-edge spectrometer. Images of the x-ray emission region were obtained using an x-ray microscope with spatial resolution of 3–5 μm and spectral bandpass of 0.6–1.7 keV, which viewed the target at $\theta = 90°$. Ion energy and spatial distributions were measured with Faraday-cup time-of-flight detectors and ion calorimeters located between $\theta = 45°$ and 135°.

In order to unravel the interrelated plasma processes, experimental results were compared with simulations using LASNEX,[6] a two-dimensional, axisymmetric, Lagrangian, fluid dynamics code. Laser-light absorption was treated using a ray tracing package, which computed refraction using a geometrical optics approximation. The representation of the laser beam shown in Fig. 1(b) was constructed from a focused fifth-power super-Gaussian, a sharp, unfocused ring, and a low-intensity background fill. The convergence angle of the ring was set at 20°. The calculations presented here assumed 9.5 J incident in a Gaussian temporal profile of 80 psec full width at half-maximum (FWHM).

Absorption via inverse bremsstrahlung was integrated along the entire ray trajectory. A simple parametrization was used to simulate the absorption behavior seen in idealized plasma simulations which account self-consistently for nonlinear density-gradient steepening at the critical surface.[7] If a given ray had a turning point at an electron density greater than a value $n_{\rm thresh}$, a fraction of its energy $f_{\rm dump}$ was absorbed at the ray's turning point. Plasma simulations at these intensities have shown density scale heights of < 1 μm at the critical surface, and suggest that $f_{\rm dump} = 0.2$–0.4 and $n_{\rm thresh} = (0.5$–$0.8)n_{\rm crit}$, as used below, except where otherwise noted.

Laser-light absorption via collective processes heated electrons by promoting particles from a Maxwellian thermal group to multiple higher-energy groups with the source function $\dot{n}_s(v) = C_c v^2 \times \exp[-v^2/2\alpha v_{\rm th}^2]$, where $v_{\rm th}$ is the mean thermal velocity of all electrons prior to heating ($v_{\rm th}^2 = kT/m$), and α is a parameter which specifies the hardness of the generated spectrum. Taking $\alpha =$ 4–6 yielded heated electron spectra consistent with plasma simulations.[7]

Electron conduction was modeled using flux-limited diffusion.[8] The energy flux transported by the electrons was constrained to be no greater than $F_{\rm max} = f_{\rm inhib} n (kT)^{3/2}/m^{1/2}$. In the usual conduction model, $f_{\rm inhib}$ was 1.2, although in practice the calculations were not sensitive to factor-of-2 changes in the flux limiter. Magnetic field physics was included using a realization of Braginskii's results.[9] Thermoelectric field generation had the form

$$\frac{\partial \vec{B}}{\partial t} = \nabla \times \left[\vec{v} \times \vec{B} + \frac{c}{en}\left(\nabla P_e - \frac{1}{c}\vec{J} \times \vec{B} - \vec{R} \right) \right] \qquad (1)$$

which gave rise to the well-known $\nabla n \times \nabla T$ term. The electron heat conduction was strongly inhibited by the fields when $\omega_{ce}\tau_{ei} \gg 1$ with an effective flux reduction factor $f_{\text{inhib}} = 4(\lambda/L)(\omega_{ce}\tau_{ei})^{-2}$, where L is the density scale height and λ the electron mean free path.

Observations of the scattered-light behavior indicate the importance of collective processes. The measured absorption fraction was 0.27 ± 0.09 at a nominal intensity of 2×10^{15} W/cm^2 and 0.41 ± 0.08 at $(3-5)\times10^{16}$ W/cm^2. Note that the trend towards increasing absorption at higher intensities must be considered tentative. The results obtained with the enclosing calorimeter show the absorption varying from 0.35 to 0.39 for the respective intensities. Analytic estimates of inverse bremsstrahlung, and more detailed calculations with LASNEX, even neglecting various nonlinear reductions, show that it falls short of producing the observed absorption fraction: by a factor of 2 at 2×10^{15} W/cm^2 and by a factor of 5 or more above 10^{16} W/cm^2. Further, the scattered-light distribution shows a polarization-dependent component. The observed ratio of intensity perpendicular to the plane of polarization to that in the plane was between 1.5 and 3.0, depending upon intensity and polar scattering angle, consistent with the presence of resonance absorption or stimulated side scatter. The observed time dependence of the reflected light collected by the focusing lens followed the incident pulse at fluxes near 10^{15} W/cm^2. However, at 2×10^{16} W/cm^2 a transient reflection pulse was observed, as shown in Fig. 2(a). The 20-psec period of enhanced reflectivity is consistent with out estimate of the persistence time of Brillouin backscatter in the low heat capacity of the corona.[10] Note, however, that both the polarization- and time-dependent behavior could be produced by other mechanisms such as varying convexity or breakup of the critical surface. The results obtained using LASNEX to calculate the azimuthally averaged scattered-light distribution are shown with the experimental results in Fig. 2(b). The agreement obtained seems adequate in view of the sensitivity of the calculation to incident energy distribution, and the simple model of absorption and scattering.

The observed x-ray spectra for the nominal 90- and 30-μm spot sizes are shown in Fig. 3. The reference calculations, using $\alpha = 4$, show the nonthermal tails evident in the data, and show the increase in high-energy emission as the intensity increases. Note that the $\alpha = 1$ calculations fall several orders of magnitude below the data at high energies. The calculation of these spectra is nontrivial, since the most intense region for 8–10-keV x-ray emission is at density 0.01 g/cm^3, while that for 1–2-keV x-rays is at density 0.1 g/cm^3. The time-varying scale height, suprathermal electron populations, and the space- and energy-dependent transport inhibition make the connection between the electron populations in the critical density region and the time-integrated x-ray spectrum quite indirect.

The spatial distribution of x-ray emission transverse to the beam axis is shown in Fig. 4 for spot sizes of 80 and 34 μm. The calculated FWHM's for the emission regions are in agreement with the experimentally observed results, within uncertainties in the beam spot size. For the 90-μm case, the code calculated a FWHM of 77 μm, while the experimental average was 67 ± 9 μm. For the 30-μm case, the calculated FWHM was 34 μm, while the experiments gave 37 ± 7 μm.

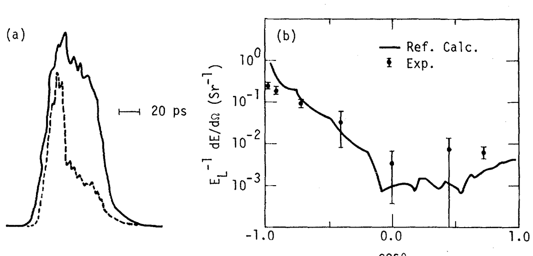

FIG. 2. Scattered light behavior: (a) incident (solid line) and reflected (dashed line) intensity versus time for a typical 30-μm shot at 2×10^{16} W/cm^2; (b) azimuthally averaged, time-integrated angular distribution, normalized by laser input energy. Experimental points show the mean and standard deviation of 30-μm shots with intensities of $(1-3)\times10^{16}$ W/cm^2.

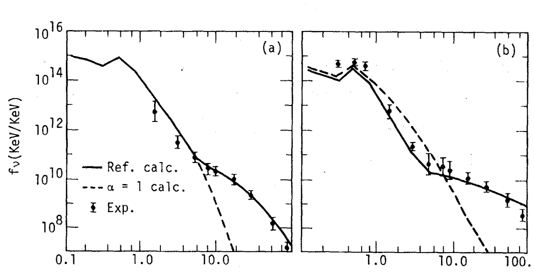

FIG. 3. X-ray emission spectra, average of experiments at (a) 90-μm spot size, with intensities of $(1-3)\times10^{15}$ W/cm^2; (b) 30-μm spot size, $(1-3)\times10^{16}$ W/cm^2. The mean and standard deviation of pulse lengths averaged are 80 ± 20 psec.

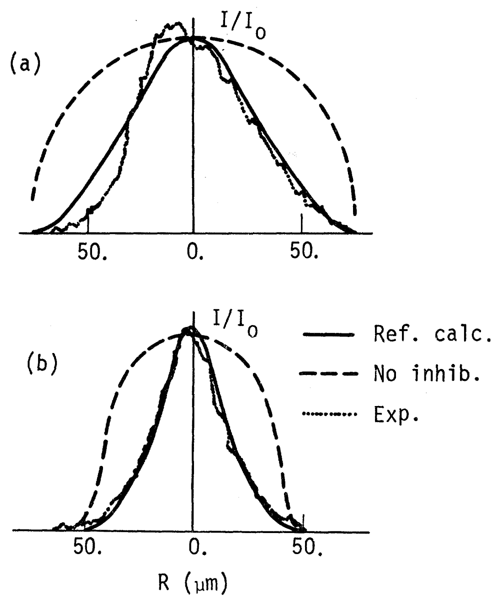

FIG. 4. X-ray spatial profiles transverse to the beam direction: (a) 80-μm spot size with 6.2-J, 60-psec pulse; (b) 34-μm spot size with 11-J, 70-psec pulse.

However, in the transverse direction, calculations without inhibited conduction (no magnetic fields or anomalous flux limit), showed FWHM's in severe disagreement with the data.

The data obtained from ion calorimetry showed ion emission strongly peaked in the forward direction, with an azimuthal dependence on polarization opposite to that of the scattered light. With the Faraday probes, which were designed to limit secondary electron effects, we found that a significant fraction of the ion energy was carried by a small group of fast ions: 50% or more of the total ion energy was carried by ions having $E/A > 10$ keV. Calculations showed similar behavior, with qualitatively similar angular and energy distributions. The simulations also indicated that the energy carried by fast ions depends strongly on both suprathermal electron populations and the amount of conduction inhibition. Currently considerable quantitative uncertainty exists in both the data and the calculations.

To determine the sensitivity of the results to details of the transport model used, calculations were performed using Bohm diffusion, and also replacing or combining magnetic field physics with an anomalous flux limit based on a model for the electron-ion two-stream instability.[11] These conduction-inhibition mechanisms produced simulation results which were similar enough to lie within uncertainties of current experimental results. However, theory indicates that the fluctuation levels generated by the instability are too small to provide such a small flux limit.[12]

The results of the present work thus show strong evidence of nonclassical absorption and transport processes. Absorption is enhanced relative to estimates of inverse bremsstrahlung. We observe polarization and time dependence of scattered light. Furthermore, only the assumption of laser generation of suprathermal electrons suffices to simulate the x-ray spectral emission. Finally, x-ray micrographs show that transport inhibition significantly modifies heat flow in the plasma.

Particular thanks are due to J. Emmett, H. Ahlstrom, L. Coleman, C. Hendricks, J. Holtzrichter, J. Nuckolls, and R. Speck for encouragement and support, and to M. Boyle, K. Estabrook, L. Koppel, R. Lerche, K. Pettipiece, H. Shay, V. Slivinsky, and G. Zimmerman for valuable contributions and discussions.

[1]G. Charatis *et al.*, in *Proceedings of the Fifth International Conference on Plasma Physics and Controlled Nuclear Fusion Research, Tokyo, Japan, 1974* (International Atomic Energy Agency, Vienna, 1975), Vol. II, p. 317; H. G. Ahlstrom *et al.*, *ibid.*, p. 375, M. Lubin *et al.*, *ibid.*, p. 459.

[2]C. Yamanaka *et al.*, Ref. 1, p. 421; B. H. Ripin *et al.*, Phys. Rev. Lett. 34, 1313 (1975); J. F. Kephart, R. P. Goodwin, and G. H. McCall, Appl. Phys. Lett. 25, 108 (1974).

[3]R. A. Haas *et al.*, University of California Report No. UCRL-77930, 1976 (to be published).

[4]Union Carbide Corp., Bound Brook, N. J.

[5]J. F. Holtzrichter and D. R. Speck, J. Appl. Phys. 47, 2459 (1976).

[6]G. B. Zimmerman, University of California Report No. UCRL-74811, 1973 (unpublished); D. S. Bailey, University of California Report No. UCRL -75881, 1974 (unpublished).

[7]K. G. Estabrook, E. J. Valeo, and W. L. Kruer, Phys. Fluids 18, 1151 (1975).

[8]E. G. Corman *et al.*, Nucl. Fusion 15, 377 (1975).

[9]S. I. Braginskii, in *Reviews of Plasma Physics*, edited by M. A. Leontovich (Consultants Bureau, New York, 1965), Vol. 1, p. 205.

[10]W. L. Kruer, E. J. Valeo, and K. G. Estabrook, Phys. Rev. Lett. 35, 1076 (1975).

[11]B. Fried and R. Gould, Phys. Fluids 4, 139 (1961); R. J. Bickerton, Nucl. Fusion 13, 457 (1973); R. C. Malone, R. L. McCrory, and R. L. Morse, Phys. Rev. Lett. 34, 721 (1975).

[12]R. W. Mitchell *et al.*, Bull. Am. Phys. Soc. 20, 1377 (1975).